High Yield Synthesis and Characterization of Chromaboranes. Comparison of the Geometric, Electronic, and Chemical Properties of an Electronically Unsaturated $(\eta^5\text{-}C_5Me_5)_2Cr_2B_4H_8$ Cluster with Its Saturated Derivative $(\eta^5\text{-}C_5Me_5)_2Cr_2(CO)_2B_4H_6$

Jianwei Ho, Kathryn J. Deck, Yasushi Nishihara, Maoyu Shang, and Thomas P. Fehlner*

Contribution from the Department of Chemistry and Biochemistry, University of Notre Dame, Notre Dame, Indiana 46556

Received June 2, 1995[⊗]

Abstract: The reaction of BH_3·THF with $[Cp^*CrCl]_2$, $Cp^* = \eta^5\text{-}C_5Me_5$, leads to the isolation of $Cp^*_2Cr_2B_4H_8$ (**1**) in very good yield. This green-brown, diamagnetic chromaborane cluster exhibits a nido geometry based on a pentagonal pyramidal deltahedron with metal atoms occupying the axial vertices and boron atoms four of the five equatorial vertices. Reaction with CO leads cleanly to brown, diamagnetic $Cp^*_2Cr_2(CO)_2B_4H_6$ (**3**) possessing the same cluster core structure as **1**. Fenske−Hall molecular orbital calculations show that both **1** and **3** have a significant Cr−Cr bonding interaction and that the cluster geometry is properly described as a bicapped tetrahedron. On this basis, **3**, with 6 cluster bonding pairs, is an electronically saturated cluster whereas **1**, with only 5 cluster bonding pairs, is unsaturated. The calculations show that it is the high energy of the Cr 3d orbitals that leads to the electronic unsaturation of **1** and that the back-bonding of the CO ligands in **3** selectively stabilizes some of the Cr metal orbitals producing an additional filled skeletal orbital. The reaction of $LiBH_4$ with $[Cp^*CrCl]_2$ results in the formation of the green-brown, paramagnetic $[Cp^*Cr(BH_4)]_2$ borohydride complex, **2**, which has been characterized spectroscopically. Chromaborane **2** reacts with stoichiometric amounts of CO at low temperature to yield brown, diamagnetic $[Cp^*Cr(CO)_2(BH_4)]_2$ (**4**). Based on the 18 electron rule, **2** is electronically unsaturated whereas **4** is saturated. The intercomparison of these four compounds is used to illustrate the structural expression of an electronically unsaturated metallaborane cluster bonding network and to relate this description to analogous organometallic compounds.

Introduction

Unsaturated compounds have always played an important role in chemistry simply because the characteristics of the associated geometric and electronic structure give rise to useful reactivity and physical properties. Unsaturation is a formal deficiency of valence electrons relative to an electronic capacity based on some bonding model. The response of a given compound to its deficiency of electrons results in observable structural characteristics. For example, multiple bonds, e.g., M=M, or multicenter bonds, e.g., BHB or CHM, are expressions of electronic unsaturation. Unsaturated clusters have similar importance in the realm of cluster chemistry,[1,2] but the number of known unsaturated clusters is small[3] and their unsaturation sometimes difficult to establish.[4]

In one sense, the term "electronically unsaturated cluster" is difficult to precisely define as the existence of cluster compounds themselves can be viewed as a structural response to a number of valence electrons insufficient to form a classical structure with two-center two-electron bonds.[5−8] Fortunately this structural response is a well-defined one, particularly for main group clusters. That is, a main group atom cluster structure is based on a closed deltahedron with n vertices where each fragment provides three frontier orbitals and together contribute $2n - 2$ electrons to framework bonding.[5] Furthermore, the addition of two cluster bonding electrons to a n-vertex closo cluster results in an open nido cluster based on a $(n + 1)$ vertex deltahedron with one unoccupied vertex. Although in a practical sense a closo cluster may be considered unsaturated relative to its nido partner, the term "unsaturated" is more properly applied to cluster systems that do not possess a sufficient number of cluster valence electrons to support the cluster geometry observed. It follows that such clusters should easily add a pair of electrons to the cluster bonding network without a qualitative change in cluster geometry.

The known unsaturated clusters all involve transition metals; however, the isolobal principle[9] provides a connection between main group and transition metal clusters, e.g., ML_3 fragments with three frontier orbitals containing two electrons, such as $Fe(CO)_3$ or CpCo ($Cp = \eta^5\text{-}C_5H_5$), exhibit a rich cluster chemistry[10,11] including the mixed metallaborane systems.[12−15] But it is also well documented that, (a) the number of ligands per fragment, (b) the steric constraints associated with cluster

[⊗] Abstract published in *Advance ACS Abstracts*, September 15, 1995.

(1) Adams, R. D.; Wang, S. *Organometallics* **1986**, *5*, 1272.
(2) Adams, R. D.; Wang, S. *Organometallics* **1987**, *6*, 739.
(3) Lavigne, G.; Kaesz, H. D. In *Metal Clusters in Catalysis*; Gates, B. C., Guczi, L., Knözinger, H., Eds.; Elsevier: Amsterdam, 1986; p 43.
(4) McCarthy, D. A.; Krause, J. A.; Shore, S. G. *J. Am. Chem. Soc.* **1990**, *112*, 8587.
(5) Wade, K. *New Scientist* **1974**, *62*, 615.
(6) Wade, K. *Adv. Inorg. Chem., Radiochem.* **1976**, *18*, 1.
(7) Mingos, D. M. P. *Acc. Chem. Res.* **1984**, *17*, 311−319.
(8) Mingos, D. M. P.; Johnston, R. L. *Struct. Bonding* **1987**, *68*, 29.
(9) Mingos, D. M. P.; Wales, D. J. *Introduction to Cluster Chemistry*; Prentice Hall: New York, 1990.
(10) Johnson, B. F. G.; Lewis, J. *Adv. Inorg. Chem. Radiochem.* **1981**, *24*, 225.
(11) *The Chemistry of Metal Cluster Complexes*; Shriver, D. F., Kaesz, H. D., Adams, R. D., Eds.; VCH: New York, 1990.
(12) Grimes, R. N. In *Metal Interactions with Boron Clusters*; Grimes, R. N., Ed.; Plenum: New York, 1982; p 269.
(13) Housecroft, C. E.; Fehlner, T. P. *Adv. Organomet. Chem.* **1982**, *21*, 57.
(14) Kennedy, J. D. *Prog. Inorg. Chem.* **1984**, *32*, 519.
(15) Kennedy, J. D. *Prog. Inorg. Chem.* **1986**, *34*, 211.

0002-7863/95/1517-10292$09.00/0

structure,[16] (c) the π donor/acceptor capabilities of the ligands,[17] (d) the actual electronic role of the so-called "t_{2g}" orbitals on the transition metal center, which are often assumed to be nonbonding in isolobal relationships,[18-20] and (e) the various expressions of the capping principle[9] increase the complexity of the relationship between structure and cluster electron count for clusters containing transition metal fragments. Thus, both the characterization of the unsaturated cluster and its structural response to the addition of an electron pair to the framework bonding are required to define the system.

Metallaboranes constitute an attractive entry point to the synthesis of additional unsaturated clusters. The large number of known compounds[12-15] provide an empirical verification of the electron counting rules and the isolobal principle. The appropriate mix of main group and transition element fragments avoids both the generally high reaction barriers of the pure main group clusters as well as the low reaction barriers of the pure transition metal clusters, i.e., usable kinetic control can be achieved. Finally, variation in the transition metal provides a means of systematically reducing the number of electrons formally contributed to cluster bonding by a given ML_n fragment.

Stimulated by the work of Messerle et al.[21] we have recently shown that the $[Cp^*CoCl]_2$ dimer, $Cp^* = \eta^5$-C_5Me_5, reacts cleanly with $[BH_4]^-$ or BH_3·THF to give cobaltaboranes,[22-24] some of which were previously observed by other routes.[12,25,26] This chemistry suggested a systematic approach to earlier transition metal analogs with a decreased number of formal cluster valence electrons. One possible response to a decreased number of valence electrons is an electronically unsaturated cluster bonding network.

Thus, we set out to make metallaboranes containing the Cp*Cr fragment. A few clusters containing boron and chromium atoms are known,[27,28] but with the exception of simple borohydrides[29] and complexes of $B_2H_4(PR_3)_2$[30] or $B_3H_8^-$,[31] chromaborane chemistry is unexplored. Of related interest, a number of molybdaboranes have been described recently including $[\{Mo(\eta\text{-}C_5H_4Me)\}_2B_5H_9]$.[32] In the following we show that the $[Cp^*CrCl]_2$ dimer reacts cleanly with monoboranes to yield both new borohydrides and chromaboranes, one of which is a true electronically unsaturated cluster.[33]

Experimental Section

General. All manipulations were carried out under a nitrogen or argon atmosphere using standard Schlenk line or drybox techniques. Solvents were predried over 4-Å molecular sieves (tetrahydrofuran, CH_2Cl_2) or KOH (hexanes, toluene) and purged with N_2 prior to distillation. Diethyl ether, tetrahydrofuran (THF), hexanes, toluene, and pentane were distilled from sodium benzophenone ketyl. Dichloromethane was distilled from CaH_2. Hydrogen (H_2) and carbon monoxide (CO) were used directly from the tank. The starting material $[Cp^*CrCl]_2$, $Cp^* = \eta^5$-(C_5Me_5),[34] was prepared according to published procedures, with the modification that the anhydrous, solid $CrCl_2$, dried by heating to 130−150 °C under vacuum for at least 2 h, was added to a stirred THF suspension of freshly prepared $[C_5Me_5]Li$ (C_5Me_5H, Lancaster; *n*-BuLi, Aldrich). The air-sensitive dimer was always used completely within 1 day of preparation as long-term storage led to decomposition. The BH_3·THF and $LiBH_4$ solutions (Aldrich) were used as received and periodically titrated.

Table 1. ^{11}B NMR of the Chromaboranes[a]

compd	δ (fwhm, Hz)	{^1H} δ (fwhm, Hz)
1	126.5 d, J = 160 Hz	126.5 s (83)
	34.3 m (264)	34.3 s (97)
2	−158 br s (1100)	
3	63.9 d, J = 88 Hz	63.9 s (100)
	34.9 m (340)	34.9 s (240)
4	54.9 tt, J = 106, 53 Hz	54.9 s (120)

[a] Hexanes at 20 °C.

Table 2. ^1H NMR of the Chromaboranes

compd	δ (fwhm, Hz)	compd	δ (fwhm, Hz)
1[a]	8.5 br (460), $2BH_t$	**3**[b]	5.2 pcq[c] (450), $2BH_t$
	3.3 br q, J_{BH} = 130 Hz, 2BHt		2.5 br (270), $2BH_t$
	1.94 s Cp*		1.80 s, Cp*
	−3.9 pcq[c] (180), 4 CrHB		−12.7 s (44), 2CrHB
2[a]	6.7 (70), Cp*	**4**[b]	6.0 pcq[c] (360), $4BH_t$
	-54.3 (1400), 4 CrHB		1.85 s, Cp*
			−12.2 pcq[c] (52), 4CrHB

[a] C_6D_6, 18 °C. [b] $CDCl_3$, 18 °C. [c] pcq = partially collapsed quartet.

NMR spectra were obtained on a Varian-300 FT- NMR spectrometer. Residual protons of solvent were used as the reference for ^1H NMR (δ, ppm: chloroform, 7.26, benzene, 7.15; dichloromethane, 5.32; toluene, 2.09). For ^{13}C NMR, solvent signals were used as the chemical shift reference, while a sealed tube containing $[(NEt_4)(B_3H_8)]$ (δ −29.7 ppm) was used as the external reference for ^{11}B NMR. Infrared spectra were obtained on a Nicolet 205 FT-IR spectrometer. Mass spectra were obtained on a Finnigan MAT Model 8400 mass spectrometer with EI and CI ionization modes. Perfluorokerosene was used as the standard for the high-resolution EI mass spectra.

Synthesis of $Cp^*_2Cr_2B_4H_8$ (1). A greenish-brown THF solution (50 mL) of $[Cp^*CrCl]_2$ (1.26 g, 2.83 mmol) was cooled to −30 °C before adding BH_3·THF (11.4 mL of a 1.0 M solution, 11.4 mmol). After being warmed slowly to ambient temperatures the solution was allowed to stir for 12 h. The THF was removed by reduced pressure, and hexane (5 mL) was added and the remaining traces of THF removed under vacuum. Hexane extraction afforded a brown solution, while bright green material, identified as $[Cp^*CrCl_2]_2$ (NMR (^1H, $CDCl_3$), δ −48 ppm (br); MS (EI) 516 ($^{12}C_{20}{}^1H_{30}{}^{35}Cl_3{}^{37}Cl^{52}Cr_2$, pattern fits 2 Cr, 4 Cl)) remained undissolved in hexane. The hexane extract was filtered and after removal of the hexane under vacuum gave an oily solid. The solid was re-dissolved in pentane (10−20 mL), and the resulting solution was concentrated for crystallization. Green-brown, air sensitive, thread-like crystals grew overnight at −4 °C and were then recrystallized from hexane. Typical yields before recrystallization were ~40% based on chromium (≈80% considering that the coproduct is $[Cp^*CrCl_2]_2$). MS (EI), P^+ = 426, 4 boron atoms, calcd for the weighted average of $^{12}C_{20}{}^1H_{38}{}^{11}B_4{}^{52}Cr_2$, $^{12}C_{20}{}^1H_{38}{}^{10}B^{11}B_3{}^{52}Cr^{53}Cr$ multiplet, 426.2172, obsd, 426.2192. Other spectroscopic data are given in Tables 1−4.

Synthesis of $Cp^*_2Cr_2(BH_4)_2$ (2). $[Cp^*CrCl]_2$ (1.60 g, 3.6 mmol) was dissolved in THF (50 mL), and the dark, green-brown solution was chilled to ca. −50 °C before $LiBH_4$ (3.6 mL, 2.0 M in THF; 7.2 mmol) was added. The mixture was warmed to room temperature. After a total reaction time of 3 h 50 min, hexane extraction with

(16) Mingos, D. M. P. *Inorg. Chem.* **1982**, *21*, 464.
(17) Chisholm, M. C.; Clark, D. L.; Hampden-Smith, M. J.; Hoffman, D. H. *Angew. Chem., Int. Ed. Engl.* **1989**, *28*, 432.
(18) Mingos, D. M. P. *J. Chem. Soc., Chem. Commun.* **1985**, 1352.
(19) Halet, J.-F.; Saillard, J.-Y. *New J. Chem.* **1987**, *11*, 315.
(20) Halet, J.-F.; Hoffmann, R.; Saillard, J.-Y. *Inorg. Chem.* **1985**, *24*, 1695.
(21) Ting, C.; Messerle, L. *J. Am. Chem. Soc.* **1989**, *111*, 3449.
(22) Deck, K. J.; Fehlner, T. P.; Rheingold, A. L. *Inorg. Chem.* **1993**, *32*, 2794.
(23) Nishihara, Y.; Deck, K. J.; Shang, M.; Fehlner, T. P. *J. Am. Chem. Soc.* **1993**, *115*, 12224.
(24) Nishihara, Y.; Deck, K. J.; Shang, M.; Fehlner, T. P.; Haggerty, B. S.; Rheingold, A. L. *Organometallics* **1994**, *13*, 4510.
(25) Grimes, R. N. *Accs. Chem. Res.* **1978**, *11*, 420.
(26) Grimes, R. N. *Pure Appl. Chem.* **1982**, *54*, 43.
(27) Oki, A.; Zhang, H.; Maguire, J. A.; Hosmane, N. S.; Ro, H.; Hatfield, W. E.; Moscherosch, M.; Kaim, W. *Organometallics* **1992**, *11*, 4202.
(28) Maynard, R. B.; Wang, Z.-T.; Sinn, E.; Grimes, R. N. *Inorg. Chem.* **1983**, *22*, 873.
(29) Marks, T. J.; Kolb, J. R. *Chem. Rev.* **1977**, *77*, 263.
(30) Shimoi, M.; Katoh, K.; Ogino, H. *J. Chem. Soc., Chem. Commun.* **1990**, 811.
(31) Guggenberger, L. J. *Inorg. Chem.* **1970**, *9*, 367.
(32) Bullick, H. J.; Brebenik, P. D.; Green, M. L. H.; Hughes, A. K.; Leach, J. B.; McGowan, P. C. *J. Chem. Soc., Dalton Trans.* **1995**, 67.
(33) Deck, K. J.; Nishihara, Y.; Shang, M.; Fehlner, T. P. *J. Am. Chem. Soc.* **1994**, *116*, 8408.
(34) Heintz, R. A.; Haggerty, B. S.; Wan, H.; Rheingold, A. L.; Theopold, K. H. *Angew. Chem., Int. Ed. Engl.* **1992**, *31*, 1077.

Table 3. ^{13}C NMR of the Chromaboranes[a]

compd	δ {^1H}	compd	δ {^1H}
1[a]	108.7, *C* CH_3	**3**[b]	237.1, CO
	12.4, *C*CH_3		104.6, *C* CH_3
2[a]	121.0, *C* CH_3 or *C*CH_3		12.0, *C*CH_3
	66.5, *C* CH_3 or *C*CH_3	**4**[b]	259.9, CO
			106.4, *C* CH_3
			9.5, *C*CH_3

[a] C_6D_6, 18 °C. [b] $CDCl_3$, 18°C.

Table 4. Selected Infrared Bands of the Chromaboranes

compd	ν BH (cm^{-1})	ν CO (cm^{-1})	compd	ν BH (cm^{-1})	ν CO (cm^{-1})
1[a]	2471 w		**3**[b]	2478 m	1914 s
	2442 w				1870 m
	2381 sh		**4**[b]	2475 w	1978 s
2[b]	2460 w			2432 w	1911 s
	2101 wbr				

[a] Pentane. [b] Hexanes.

filtration through Celite was carried out, to yield crude product (1.39 g, 3.45 mmol $[Cp^*Cr(BH_4)]_2$, 95%). Caution: The residue remaining from the reaction is very active. It was deactivated by making a toluene slurry and adding it dropwise into a container of acetone. The hexane extract was again filtered and the green-brown solution was concentrated slowly until many crystals began forming. It was then placed in a −40 °C freezer. Within 24 h, a crop of dark, green-black, highly air sensitive crystals was isolated (510 mg, 1.26 mmol $[Cp^*Cr(BH_4)]_2$, 35%). For mass-spectral analysis, crystals were loaded in the drybox into small crucibles with covers containing a pinhole. Each crucible was in turn placed in a dry vial under prepurified N_2 (inside the drybox) and was quickly removed from the vial immediately before measurement. MS (EI), $P^+ - H_2 = 402$, 2 boron atoms, 2 Cr atoms. Attempts to measure the mass spectrum of $[Cp^*Cr(BH_4)]_2$ under normal conditions only gave large signals due to Cp^*_2Cr and the oxo-cubane $[Cp^*Cr(\mu_3\text{-}O)]_4$.[35] Other spectroscopic data are given in Tables 1−4.

To study its thermal decomposition, a toluene solution of **2** (327 mg, 0.80 mmol) was heated at ca. 80 °C for 2 h, during which time the dark-green color gave way to brown. Hexane extraction gave a brown filtrate (>300 mg) with almost no residue remaining. The ^{11}B and ^1H NMR spectra revealed complete conversion to diamagnetic **1** and an unidentified paramagnetic coproduct not containing boron (^1H NMR, δ −16 and −26 in a 1:1 ratio). The combined intensities of the paramagnetic proton signals are about equal to that for the Cp* ligand of **1** suggesting a disproportionation reaction of **2** that leads to **1** and a complex Cp*CrH species.

Synthesis of $Cp^*_2Cr_2(CO)_2B_4H_6$ (3). CO gas at 1 atm of pressure was bubbled through a hexane solution of 0.45 g (1.06 mmol) of **1** for 1 h at room temperature. The reaction flask was then closed off and stirred for ca. 12 h. This was repeated until the ^{11}B NMR of an aliquot showed the absence of **1**. Compound **3** is considerably less soluble in hexane than **1** and forms a brown precipitate which is filtered through Celite. A toluene solution of this precipitate shows only the resonances of **3** (yield 0.45 g, 89%). Compound **3** is not as air sensitive as **1** and X-ray quality crystals were obtained by diffusing hexane into the toluene solution at ambient temperature. MS (EI), apparent $P^+ = 480$, 4 boron atoms, loss of 2 CO, calcd for the weighted average of $^{12}C_{22}{}^1H_{36}{}^{16}O_2{}^{11}B_4$-$^{52}Cr_2$, $^{12}C_{22}{}^1H_{36}{}^{16}O_2{}^{10}B^{11}B_3{}^{52}Cr^{53}Cr$ multiplet, 480.1914, obsd, 480.1925. Anal. Calcd for $C_{22}H_{36}O_2B_4Cr_2$: C, 55.08; H, 7.56. Obsd: C, 54.89; H, 7.42. Other spectroscopic data are given in Tables 1−4.

Synthesis of $Cp^*_2Cr_2(CO)_4(BH_4)_2$ (4). CO gas at 1 atm of pressure was bubbled through a hexane solution of 0.55 g (1.07 mmol) **2** at −30 °C for 5 min. The solution was filtered through Celite and a concentrated solution was stored at low temperature. An air-sensitive, apparently crystalline material precipitated but was never found to be suitable for an X-ray diffraction study. In the cases when single crystals were found, evidence of decomposition was present and the crystalline material was either $[Cp^*Cr(CO)_2]_2$ or another decomposition product with a disordered structure. Longer times and/or higher temperatures result in the formation of significant amounts of decomposition products. For example, after 30 min of reaction at 0 °C $[Cp^*Cr(CO)_2]_2$ was observable in the IR[36] and dark blue crystals of $[Cp^*Cr(CO)_2]_2$ formed from the solution after 2 h at room temperature. MS (CI, isobutane): $P^+ - 1 = 515$, 2 boron and 2 Cr; −2CO. The base peak was $P^+ - Cp^*Cr(CO)_2BH_4 - 1$. Other spectroscopic data are given in Tables 1−4.

X-ray Structure Determinations. $Cp^*_2Cr_2B_4H_8$ (1). Crystals of moderate quality were grown by slow cooling of a hexane solution of $[(Cp^*Cr)_2B_4H_8]$. A single crystal was mounted in a capillary. Crystallographic data for **1**: $C_{20}H_{38}Cr_2B_4$, tetragonal, $P4_2/n$, $a = b = 23.720(1)$ Å, $c = 8.4046(7)$ Å, $V = 4728.8(5)$ Å^3, $z = 8$, $d_{calcd} = 1.509$ g cm^{-3}. Of 3341 reflections collected on a CAD4 diffractometer, 3240 were unique and 1574 were unique observed (F_o^2) > 3.0 $\sigma(F_o^2)$. Hydrogen atoms were located but not refined in the final refinement. $R(F) = \Sigma|F_o - F_c|/\Sigma|F_o| = 6.72\%$, $R(wF) = (\Sigma w(F_o - F_c)^2/\Sigma w(F_o)^2)^{1/2} = 8.90\%$. Coordinates and selected bond distances are given in Tables 5 (supporting information) and 6, respectively. Other data were deposited in conjunction with the original communication.[33]

$Cp^*_2Cr_2(CO)_2B_4H_6$ (3). A black block-shaped crystal of **3** was mounted on a glass fiber. Crystallographic data for **3**: $C_{22}H_{36}Cr_2B_4O_2$, tetragonal, $P4_12_12$, $a = b$ 8.812(1) Å, $c = 31.147(6)$ Å, $V = 2418.6(5)$ Å^3, $z = 4$, $d_{calcd} = 1.317$ g cm^{-3}. Of 1989 reflections collected on a CAD4 diffractometer, 1676 were unique and 1294 were unique observed (F_o^2) > 3.0 $\sigma(F_o^2)$. Hydrogen atoms were not located. $R(F) = 5.50\%$, $R(wF) = 6.96\%$. Coordinates and selected bond distances are given in Tables 7 (supporting information) and 8, respectively.

MO Calculations. Fenske−Hall calculations[37,38] were carried out on $Cp_2Cr_2B_4H_8$ (**1a**), Cp = η^5-C_5H_5, as a model of $Cp^*_2Cr_2B_4H_8$ (**1**). The minimal AO basis set calculations were transformed into a fragment basis set for 2 CpCr and B_4H_8 fragments. The geometry used was that derived from the solid state structure determination of **1**. As the positions of the hydrogen atoms were not well determined in the structure solution, idealized positions were chosen using B−H and M−H−B metrics based on known metallaboranes. For comparison, calculations were carried out on $Cp_2Co_2B_4H_8$ with the same geometry. Although this is an unknown molecule, it is one which has a known analog, $Cp_2Co_2B_2H_2S_2$.[39] Calculations were also carried out on $Cp_2Cr_2(CO)_2B_4H_6$ (**3a**), as a model of $Cp^*_2Cr_2(CO)_2B_4H_6$ (**3**). In this case, transformation into a fragment basis set for the three fragments 2 CpCrCO and B_4H_6 was carried out. The hydrogen atoms were not found in the structure determination of **3** and, thus, calculations were carried out on two model systems. In one, the two appropriate Cr−H−B bridging hydrogens were removed from structure **1a** and CO ligands added as found experimentally in **1**. In the other, the H−B−H and B−B−H angles around the BH_3 fragments were adjusted to give the boron atom an approximately tetrahedral environment. The results were qualitatively the same in both cases. As the latter had more favorable nonbonding H atom contacts, a somewhat higher HOMO-LUMO gap was found. It is these calculations that are discussed below. Note that the differences in framework geometry between **1** and **3** are relatively minor ones.

Results

Synthesis and Characterization. The results of the individual reactions of $[BH_4]^-$ and BH_3·THF with $[Cp^*CrCl]_2$ or $[Cp^*CrCl_2]_2$ are summarized in Scheme 1 along with the observed reactions of the principal chromaborane products. The structures shown are based on the analyses of the spectroscopic and crystallographic data that follow.

$Cp^*_2Cr_2B_4H_8$ (1). The reaction of BH_3·THF with $[Cp^*CrCl]_2$ leads to a single boron containing compound and $[Cp^*CrCl_2]_2$. The mass spectral data give a composition $Cp^*_2Cr_2B_4H_8$ and the NMR data suggest a diamagnetic compound. The ^{11}B NMR

(35) Bottomley, F.; Chen, J.; MacIntosh, S. M.; Thompson, R. C. *Organometallics* **1991**, *10*, 907.

(36) Potenza, J.; Giordano, P.; Mastropaolo, D.; Efraty, A. *Inorg. Chem.* **1974**, *13*, 2540.

(37) Fenske, R. F. *Pure Appl. Chem.* **1988**, *27*, 61.

(38) Hall, M. B.; Fenske, R. F. *Inorg. Chem.* **1972**, *11*, 768.

(39) Micciche, R. P.; Carroll, P. J.; Sneddon, L. G. *Organometallics* **1985**, *4*, 1619.

Table 6. Selected Interatomic Distances (Å) and Angles (deg) for $Cp^*_2Cr_2B_4H_8$ (**1**)

	Distance		
Cr(1)−Cr(2)	2.870(2)	Cr(1)−B(3)	2.01(2)
Cr(1)−C(1)	2.20(1)	Cr(1)−B(4)	2.11(2)
Cr(1)−C(2)	2.20(1)	Cr(2)−C(11)	2.209(9)
Cr(1)−C(3)	2.18(1)	Cr(2)−C(12)	2.17(1)
Cr(1)−C(4)	2.19(1)	Cr(2)−C(13)	2.18(1)
Cr(1)−C(5)	2.225(9)	Cr(2)−C(14)	2.16(1)
Cr(1)−B(1)	2.13(2)	Cr(2)−C(15)	2.15(1)
Cr(1)−B(2)	2.01(2)	Cr(2)−B(1)	2.15(2)
Cr(2)−B(2)	2.02(1)	B(1)−B(2)	1.75(3)
Cr(2)−B(3)	2.04(2)	B(2)−B(3)	1.75(3)
Cr(2)−B(4)	2.12(2)	B(3)−B(4)	1.61(3)
	Angle		
C(1)−Cr(1)−B(1)	157.3(6)	C(4)−Cr(1)−B(1)	103.4(6)
C(1)−Cr(1)−B(2)	114.0(5)	C(4)−Cr(1)−B(2)	105.1(5)
C(1)−Cr(1)−B(3)	90.4(5)	C(4)−Cr(1)−B(3)	135.0(6)
C(1)−Cr(1)−B(4)	104.8(7)	C(4)−Cr(1)−B(4)	165.6(7)
C(2)−Cr(1)−B(1)	153.5(6)	C(5)−Cr(1)−B(1)	120.6(6)
C(2)−Cr(1)−B(2)	151.3(5)	C(5)−Cr(1)−B(2)	91.5(5)
C(2)−Cr(1)−B(3)	117.3(5)	C(5)−Cr(1)−B(3)	99.4(6)
C(2)−Cr(1)−B(4)	104.0(7)	C(5)−Cr(1)−B(4)	135.0(6)
C(3)−Cr(1)−B(1)	117.5(6)	B(1)−Cr(1)−B(2)	49.9(7)
C(3)−Cr(1)−B(2)	141.7(5)	B(1)−Cr(1)−B(3)	88.8(7)
C(3)−Cr(1)−B(3)	153.0(5)	B(1)−Cr(1)−B(4)	90.8(8)
C(3)−Cr(1)−B(4)	132.7(6)	B(2)−Cr(1)−B(3)	51.7(7)
C(13)−Cr(2)−B(3)	142.6(6)	B(3)−Cr(2)−B(4)	45.4(7)
C(13)−Cr(2)−B(4)	160.2(7)	C(2)−C(1)−C(5)	108.3(9)
C(14)−Cr(2)−B(1)	127.2(6)	C(1)−C(2)−C(3)	108.1(9)
C(14)−Cr(2)−B(2)	150.0(6)	C(2)−C(3)−C(4)	107.4(8)
C(14)−Cr(2)−B(3)	145.6(6)	C(3)−C(4)−C(5)	109.6(8)
C(14)−Cr(2)−B(4)	124.1(6)	C(1)−C(5)−C(4)	106.6(8)
C(15)−Cr(2)−B(1)	159.3(6)	C(12)−C(11)−C(15)	108(1)
C(15)−Cr(2)−B(2)	147.1(5)	C(11)−C(12)−C(13)	103.3(9)
C(15)−Cr(2)−B(3)	113.3(6)	C(12)−C(13)−C(14)	102.8(9)
C(15)−Cr(2)−B(4)	102.1(6)	C(13)−C(14)−C(15)	111(1)
B(1)−Cr(2)−B(2)	49.6(7)	C(11)−C(15)−C(14)	115(1)
B(1)−Cr(2)−B(3)	87.2(7)	Cr(1)−B(1)−Cr(2)	84.3(7)
B(1)−Cr(2)−B(4)	89.9(8)	Cr(1)−B(1)−B(2)	61.7(3)
B(2)−Cr(2)−B(3)	51.2(7)	Cr(2)−B(1)−B(2)	61.2(8)
B(2)−Cr(2)−B(4)	85.3(8)	Cr(1)−B(2)−Cr(2)	90.8(6)
Cr(1)−B(2)−B(1)	68.3(8)	B(2)−Cr(1)−B(4)	85.6(7)
Cr(1)−B(2)−B(3)	63.9(8)	B(3)−Cr(1)−B(4)	45.9(7)
Cr(2)−B(2)−B(1)	69.2(8)	C(11)−Cr(2)−B(1)	155.3(6)
Cr(2)−B(2)−B(3)	65.2(8)	C(11)−Cr(2)−B(2)	111.8(5)
B(1)−B(2)−B(3)	111(1)	C(11)−Cr(2)−B(3)	90.6(5)
Cr(1)−B(3)−Cr(2)	90.2(6)	C(11)−Cr(2)−B(4)	105.9(6)
Cr(1)−B(3)−B(2)	64.4(7)	C(12)−Cr(2)−B(1)	120.6(6)
Cr(1)−B(3)−B(4)	70.5(9)	C(12)−Cr(2)−B(2)	92.4(5)
Cr(2)−B(3)−B(2)	63.6(7)	C(12)−Cr(2)−B(3)	102.0(5)
Cr(2)−B(3)−B(4)	70(1)	C(12)−Cr(2)−B(4)	136.7(6)
B(2)−B(3)−B(4)	113(1)	C(13)−Cr(2)−B(1)	107.1(6)
Cr(1)−B(4)−Cr(2)	85.3(8)	C(13)−Cr(2)−B(2)	113.3(7)
Cr(1)−B(4)−B(3)	63.6(9)		
Cr(2)−B(4)−B(3)	65(1)		

spectrum indicates two distinct boron environments and the ^1H NMR spectrum indicates one Cp* (area 15) environment, which is confirmed by the ^{13}C spectrum, one BHCr (area 2) environment, and two BH (area 1 each) terminal environments. The four bridging hydrogens are associated with the high field boron signal exhibiting the more complicated coupling pattern. This is consistent with the observation that boron in borane-like environments tends to resonate at higher field than boron in metallic environments.[40] If not fluxional, the structure of **1** must contain at least one plane or 2-fold axis of symmetry. Several possibilities exist including a dibridged dichromium structure[33] analogous to $Cp^*_2Ta_2(B_2H_6)_2$.[21]

The single-crystal X-ray diffraction study of **1** revealed the core structure and suggests (located but not refined) positions for the hydrogen atoms fully consistent with the solution NMR data (Figure 1). Ostensibly the structure constitutes a nido cage as its geometry can be derived from a pentagonal bipyramid by removing one equatorial vertex. The chromium atoms occupy the axial positions and the boron atoms occupy four of the five equatorial positions. All the B−B and B−Cr distances are reasonable for such a cluster network. As often observed for nido borane structures, the bridging hydrogens occupy the edges of the open face. The Cp* ligands are not parallel and are tilted away from the open face (included angle = 28.1(8)°). The cluster electron count required for this geometry is 16; however, only 10 are available in **1** if Cp*Cr is treated as a formal −1 electron donor to cluster bonding.

The Cr-Cr distance of 2.870(2) Å in **1** does not rule out the possibility of a metal−metal bond, i.e., it is shorter than the 3.281(1) Å bonding Cr−Cr distance in $[Cp^*Cr(CO)_3]_2$[41] but longer than the average nonbonded 2.715 Å Cr−Cr distance in $[CpCrH]_4$.[34,42] If there is a Cr−Cr bond, then the cluster can be considered a bicapped tetrahedron which requires 12 cluster bonding electrons. The question of the existence of Cr−Cr bonding is discussed further below on the basis of molecular orbital (MO) calculations but it is clear that, however one counts the electrons, **1** must be considered electron deficient.

$Cp^*_2Cr_2(BH_4)_2$ (2). The reaction of $LiBH_4$ with $[Cp^*CrCl]_2$ produces a single boron containing compound in high yield which subsequently can be converted to **1** by heating. The mass spectrum suggests a minimal composition of $Cp^*_2Cr_2B_2H_6$ and the NMR data show that the compound is paramagnetic. The ^{11}B NMR signal is dramatically shifted from the normal range for diamagnetic compounds and is extremely broad (fwhm =

Table 8. Selected Interatomic Distances (Å) and Angles (deg) for $Cp^*_2Cr_2(CO)_2B_4H_6$ (**3**)

	Distance		
Cr−Cr′	2.792(1)	Cr−C(3)	2.205(9)
Cr−B(1)	2.17(1)	Cr−C(4)	2.196(8)
Cr−B(1)′	2.16(1)	Cr−C(5)	2.192(9)
Cr−B(2)	2.11(1)	Cr−C(11)	1.817(8)
Cr−B(2)′	2.13(1)	B(1)−B(2)	1.66(2)
Cr−C(1)	2.181(8)	B(2)−B(2)′	1.63(2)
Cr−C(2)	2.188(7)	C(3)−C(4)	1.41(1)
C(1)−C(2)	1.40(1)	C(4)−C(5)	1.41(2)
C(1)−C(5)	1.34(1)	C(11)−O	1.16(1)
C(2)−C(3)	1.34(1)		
	Angle		
B(1)−Cr−B(1)′	99.5(4)	B(2)′−Cr−C(2)	137.8(4)
B(1)−Cr−B(2)	45.6(4)	B(2)′−Cr−C(3)	102.5(4)
B(1)−Cr−B(2)′	83.1(4)	B(2)′−Cr−C(4)	86.8(4)
B(1)−Cr−C(1)	128.4(3)	Cr−B(1)−Cr′	80.4(4)
B(1)−Cr−C(2)	97.6(3)	Cr−B(1)−B(2)	65.4(5)
B(1)−Cr−C(3)	98.5(4)	Cr−B(1)′−B(2)	66.4(5)
B(1)−Cr−C(4)	130.5(4)	Cr−B(2)−Cr′	82.2(4)
B(1)−Cr−C(5)	158.8(3)	Cr−B(2)−B(1)	69.0(5)
B(1)−Cr−C(11)	64.8(4)	Cr−B(2)−B(2)′	68.1(5)
B(1)′−Cr−B(2)	83.8(5)	Cr′−B(2)−B(1)	68.1(5)
B(1)′−Cr−B(2)	45.6(5)	Cr′−B(2)−B(2)′	66.7(5)
B(1)′−Cr−C(1)	127.2(4)	B(1)−B(2)−B(2)′	120.3(8)
B(1)′−Cr−C(2)	162.8(4)	C(2)−C(1)−C(5)	109.7(7)
B(1)′−Cr−C(5)	101.2(4)	C(1)−C(2)−C(3)	108.5(7)
B(1)′−Cr−C(11)	100.7(4)	C(2)−C(3)−C(4)	107.4(8)
B(2)−Cr−B(2)′	45.1(4)	C(3)−C(4)−C(5)	107.8(8)
B(2)−Cr−C(1)	144.2(4)	B(1)′−Cr−C(3)	140.1(4)
B(2)−Cr−C(2)	108.6(4)	B(1)′−Cr−C(4)	107.0(4)
B(2)−Cr−C(3)	83.9(4)	B(2)′−Cr−C(5)	109.0(4)
B(2)−Cr−C(4)	96.4(5)	B(2)′−Cr−C(11)	129.5(4)
B(2)−Cr−C(5)	133.3(4)	C(1)−C(5)−C(4)	106.6(8)
B(2)−Cr−C(11)	109.7(4)	Cr−C(11)−O	172.2(8)
B(2)′−Cr−C(1)	144.2(3)		

(40) Rath, N. P.; Fehlner, T. P. *J. Am. Chem. Soc.* **1988**, *110*, 5345.

(41) Adams, R. D.; Collins, D. E.; Cotton, F. A. *J. Am. Chem. Soc.* **1974**, *96*, 749.

(42) Heintz, R. A.; Ostrander, R. L.; Rheingold, A. L.; Theopold, K. H. *J. Am. Chem. Soc.* **1994**, *116*, 11387.

Scheme 1

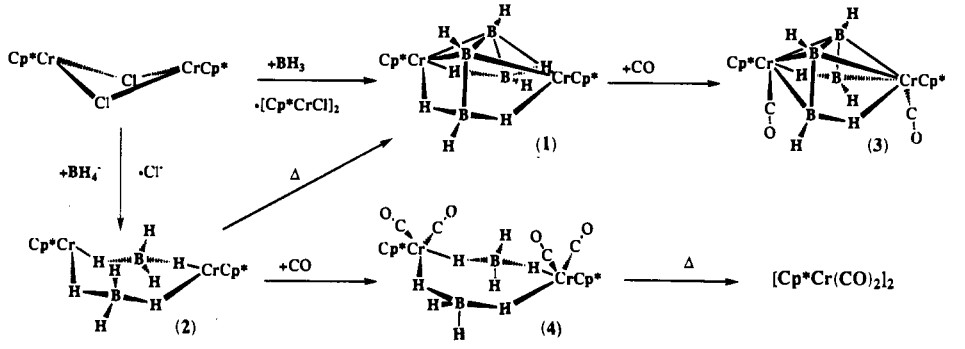

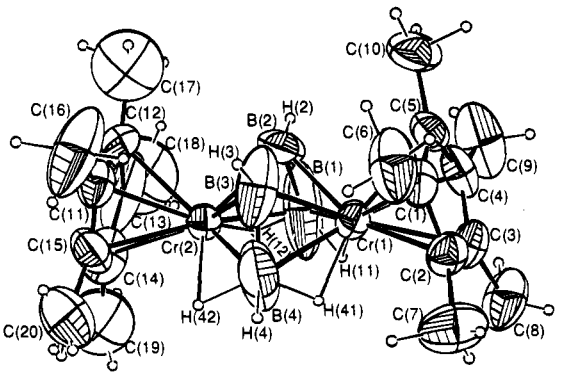

Figure 1. ORTEP drawing of the structure of $Cp^*_2Cr_2B_4H_8$ (**1**) with 40% thermal elipsoids for the heavy atoms and with arbitrarily small radii assigned to the hydrogen atoms.

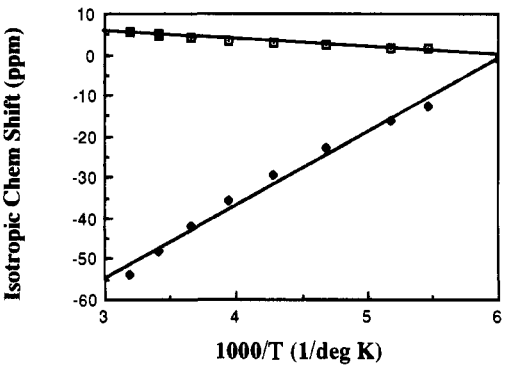

Figure 2. Plot of isotropic chemical shifts of the Cp* (open squares) and BH (solid diamonds) ^{1}H NMR signals for $Cp^*_2Cr_2(BH_4)_2$ (**2**) vs. $1/T$.

1100 Hz). The two broad ^{1}H NMR signals reveal one kind of Cp* and an average environment for several BH/BHM protons. Both ^{1}H signals are shifted from the range expected for diamagnetic compounds. Variable-temperature ^{1}H NMR studies (from −90 to +40 °C) show a temperature dependence of the chemical shifts represented by the equations:

$$\delta_{Cp^*} = (3.26 \times 10^{-2}\ \text{ppm/K})(T) - 2.74\ \text{ppm}$$

$$\delta_{BH4} = (-0.318\ \text{ppm/K})(T) + 38.2\ \text{ppm}$$

Both ^{1}H NMR signals narrow, and their chemical shifts approach the "normal" range expected for diamagnetic compounds as the temperature is lowered. Extrapolation of the Cp* data, to a typical δ_{Cp^*} (1.9 ppm), gives a δ_{BH} of −7.0 ppm. Such a chemical shift is characteristic of a fluxional borohydride ligand and is the weighted average of the shifts of the terminal and bridging protons.[29] The ^{13}C{^{1}H} NMR signals for ring and methyl carbons of Cp* are also paramagnetically shifted and are of equal intensity as the paramagnetic chromium center efficiently relaxes the ring carbons of Cp*.

The VT-NMR data suggest an equilibrium between high- and low-spin states and a standard treatment of the data was carried out.[43] Using δ 1.9 ppm as the diamagnetic shift for Cp*, and the extrapolated chemical shift value (−7.0 ppm) as the diamagnetic shift for BH_4, allows a calculation of the isotropic (or paramagnetic) chemical shifts. A plot of the isotropic chemical shifts against the reciprocal of the absolute temperature gives straight lines (Figure 2) as expected for Curie law behavior.[44]

The strong IR absorption at 2460 cm^{-1} is assigned to a BH_t stretching mode and the weak, broad band at 2102 cm^{-1} to a BHM bridging mode. These IR absorptions are consistent with the presence of either bidentate or tridentate borohydride ligands.[29]

Although we were unable to obtain satisfactory single crystals, this paramagnetic chromaborane is formulated as $[Cp^*Cr(BH_4)]_2$. The data are consistent with a simple displacement of the Cl$^-$ ligands of paramagnetic $[Cp^*CrCl]_2$ by the pseudohalide BH_4^-. The eighteen-electron, diamagnetic complex $[PPN]^+[(\mu\text{-}H)_2BH_2Cr(CO)_4]^-$ is known[45] and the borohydride ligand gives a single ^{1}H NMR signal at δ −9.5 ppm close to that extrapolated for the borohydride ligand in **2**. Structurally characterized examples of both bi- and tridentate μ_2-BH_4 complexes exist, e.g., the (μ_2:η^2-BH_4) complex $[(C_5CH_3)_5Ir]_2H_3BH_4$[46] and the (μ_2:η^3-BH_4) complex $Co_2(BH_4)_2(Ph_2P[CH_2]_5PPh_2)_2$.[47] Note that **2** is isoelectronic with the paramagnetic $[Cp^*CrMe]_2$ dimer and that the organometallic compound is viewed as electron deficient.[34,42]

When $[Cp^*Cr(BH_4)]_2$ is heated it gives rise to a single diamagnetic product, **1**, and an unidentified paramagnetic product (or products). The latter has Cp*, Cr, and hydride components suggesting a ligand disproportionation reaction but the nature of the decomposition mechanism is unclear. The reaction of $[Cp^*CrBH_4]_2$ with 2 BH_3·THF gave intractable products and no trace of **1**.

$Cp^*_2Cr_2(CO)_2B_4H_6$ (3). The reaction of **1** with CO yields two boron-containing products. The ^{11}B NMR spectra as a function of reaction time suggest parallel paths to yield **3** (89%) and an unknown second product (≈5%) in that long reaction times showed no interconversion of the two species. The mass spectral data give a composition of $Cp^*_2Cr_2(CO)_2B_4H_6$ and the NMR data suggest a diamagnetic compound. The ^{11}B NMR

(43) Satterlee, J. D. *Concepts Magn. Reson.* **1990**, *2*, 69.

(44) Jesson, J. P. In *NMR of Paramagnetic Molecules*; LaMar, G. N., Horrocks, W. DeW., Jr., R. H. Holm, R. H., Ed.; Academic: New York, 1973; p 1.

(45) Darensbourg, M.; Bau, R.; Marks, M.; Burch, R. R., Jr.; Deaton, J. C.; Slater, S. *J. Am. Chem. Soc.* **1982**, *104*, 6961.

(46) Gilbert, T. M.; Hollander, F. J.; Bergman, R. G. *J. Am. Chem. Soc.* **1985**, *107*, 3508.

(47) Holah, D. G.; Hughes, A. N.; Maciaszek, S.; Magnuson, V. R. *J. Chem. Soc., Chem. Commun.* **1983**, 1308.

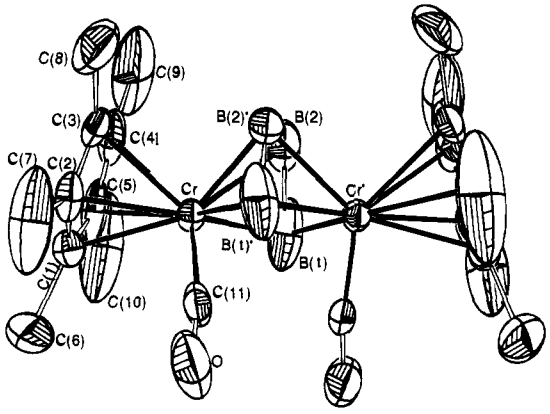

Figure 3. ORTEP drawing of the structure of $Cp^*_2Cr_2(CO)_2B_4H_6$ (**3**) with 40% thermal elipsoids for the heavy atoms.

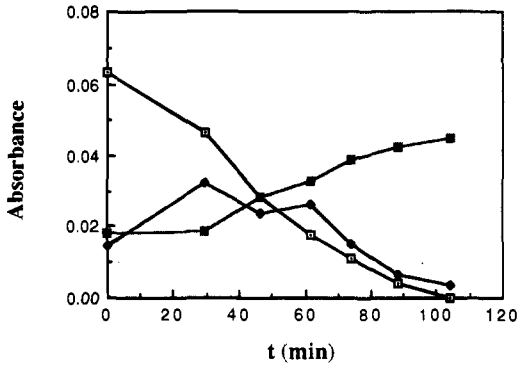

Figure 4. Plot of characteristic IR absorbances for **4** (1978.3 cm^{-1}, open squares), $[Cp^*Cr(CO)_2]_2$ (1857.6 cm^{-1}, solid squares), and $Cp^*CrH(CO)_3$ (1921.2 cm^{-1}, solid diamonds) as a function of time on heating at 50 °C.

spectrum indicates two distinct boron environments and the ^1H NMR spectrum indicates one Cp* (area 15) environment which is confirmed by the ^{13}C spectrum, one BHCr (area 1) environment, and two BH (area 1 each) terminal environments. The two bridging hydrogens are associated with the high-field boron signal. Comparison of the NMR data for **1** and **3** suggests similar framework structures even though other possibilities exist. The IR data are of particular interest. A single BH stretching frequency is observed plus two intense absorptions not present in **1** that are assigned to CO stretching frequencies. The frequencies are consistent with terminal CO's and the ^{13}C NMR data require equivalent CO ligands for a static structure. Two bands are observed because of coupling between the two stretching modes and the relative intensities permit the dihedral angle between them to be estimated as 60° vs. 49° in the solid state (see below).[48] The low-field ^{13}C chemical shift and low-frequency CO stretching vibrations relative to, e.g., Fe−CO, suggest significant Cr to CO π-back-bonding.[49,50]

A single-crystal X-ray diffraction study of **3** shows that the core structure (Figure 3) is indeed very similar to that of **1**. The hydrogen atoms were not located; however, the spectroscopic data place them unambiguously as shown in Scheme 1. Despite the fact that **3** has two more skeletal electrons than **1** (2 CO molecules added, 2 H lost), the cage retains the apparent nido structure observed for **1** (the required cluster electron count is 16 but only 12 are available). Again the B−B and B−Cr distances are reasonable for a cluster network and, as in **1**, the Cp* ligands are tilted away from the open face (included angle = 30.4(20)°) and the Cr−Cr distance (2.792(1) Å) may or may not be bonding. Note that, if the Cr−Cr interaction is a bonding one, the cluster can be considered a bicapped tetrahedron and would formally satisfy the electron counting rules, i.e., it would be saturated.

$Cp^*_2Cr_2(CO)_4(BH_4)_2$ (4). The reaction of **2** with CO is extremely rapid; however, at low temperature and short reaction times a single product is obtained. Only CI-MS was successful and the $P^+ - 1$ ion, although low in intensity, was real as judged by comparison of mass chromatograms of the various fragment ions. The isotope distribution pattern of the $P^+ - 1$ ion was consistent with a compound containing 4 boron and 2 Cr atoms. In contrast to **2**, the NMR data suggest a diamagnetic compound as all of the chemical shifts and peak widths are normal. A single boron resonance is seen and it is at very low field relative to mononuclear borohydride complexes. Selective ^1H decoupling demonstrates that this resonance is a triplet of triplets which is assigned to a $(\mu\text{-H})_2BH_2$ ligand. Only a single Cp* resonance is seen in the ^1H NMR and the distinct, equal intensity terminal and bridging ^1H resonances verify bidentate $(\mu\text{-H})_2BH_2$ ligand coordination and a nonfluxional borohydride ligand. The single ^{13}C NMR resonance of the CO ligands combined with the observation of only two absorptions in the CO stretching region in the IR suggests equivalent terminal CO ligands on adjacent Cr metal centers with vibrational coupling and π-back-bonding similar to that observed for **3**. In the absence of a solid state structure determination, a fluxional structure cannot be completely ruled out but a static structure seems most likely. Hence, a structure of **4** possessing effective C_{2v} symmetry is postulated and shown in Scheme 1.

With this formulation of its structure, **4** is related to $Cp^*CrH(CO)_3$ in the sense that each bridging BH_4 ligand replaces one CO ligand in the coordination sphere of one Cr atom and the H atom in the other. Thus, each Cr atom in **4** obeys the 18 electron rule and it may be considered the saturated partner of **2**. In contrast to **2** which is paramagnetic, **4** is diamagnetic. The even number of electrons at each d^4 metal center combined with the differential stabilization of the metal based valence functions by the CO ligands (see also below) presumably results in a large HOMO-LUMO gap for the dimer.

Heating a hexane solution of **4** under Ar at 50 °C did not lead to **3**. The reaction progress was monitored using the absorbances of **4**, $[Cp^*Cr(CO)_2]_2$, and $Cp^*CrH(CO)_3$[51] to monitor concentration changes. The results, Figure 4, show a time dependence of $Cp^*CrH(CO)_3$ characteristic of an intermediate and a time dependence of $[Cp^*Cr(CO)_2]_2$ characteristic of a product. Presumably the boron is lost as B_2H_6 or BH_3CO.

Product **4** is not observed in the reaction of **2** with excess CO at room temperature and/or with long reaction times. Instead only $[Cp^*Cr(CO)_2]_2$, $Cp^*CrH(CO)_3$, and other unidentified boron free products are observed. The reaction of **2** with excess PPh_3 gave BH_3PPh_3 by ^{11}B NMR which is consistent with the formation of BH_3CO plus the metal hydride in the reaction of **2** with excess CO or at long times. Thus, base displacement of BH_3, a reaction typical of borohydrides, is competitive with coordination at the metal center.

Molecular Orbital Calculations. One important point on which the structural data are ambiguous is whether or not a significant Cr−Cr bonding interaction exists in **1** and **3**. The molecular orbital (MO) calculations suggest that one does. MO correlation diagrams for **1a** and **3a** are given in Figures 5 and 6. Both compounds show similar HOMO energies, i.e., reasonable theoretical ionization potentials, and significant

(48) Cotton, F. A.; Wilkinson, G. *Advanced Inorganic Chemistry*, 3rd ed.; John Wiley: New York, 1972.
(49) Gardner, T. G.; Girolami, G. S. *Organometallics* **1987**, *6*, 2551.
(50) Morris, R. J.; Girolami, G. S. *Inorg. Chem.* **1990**, *21*, 4167.
(51) Jaeger, T. J.; Baird, M. C. *Organometallics* **1988**, *7*, 2074.

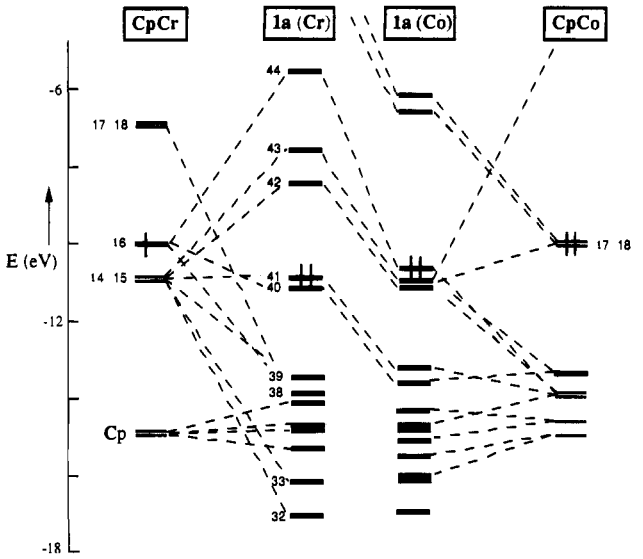

Figure 5. Comparison of the Fenske–Hall MO diagrams of $Cp_2Cr_2B_4H_8$ (**1a**) and $Cp_2Co_2B_4H_8$ showing their relationship to the frontier orbitals of the CpCr and CrCo fragments, respectively.

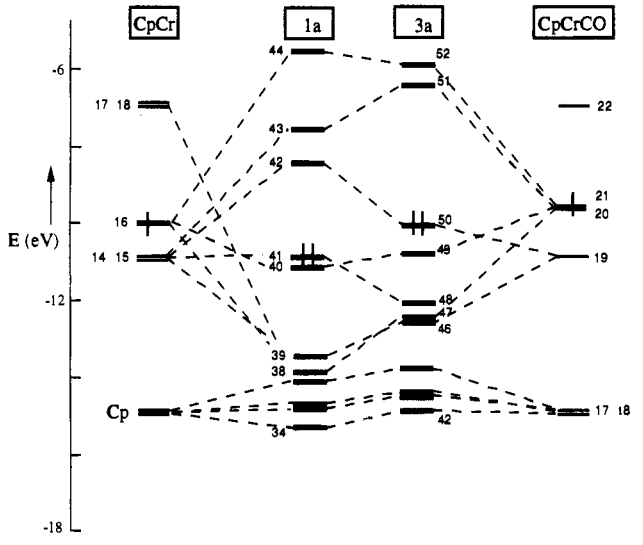

Figure 6. Comparison of the Fenske–Hall MO diagrams of $Cp_2Cr_2B_4H_8$ (**1a**) and $Cp_2Cr_2(CO)_2B_4H_6$ (**3a**) showing their relationship to the frontier orbitals of the CpCr and CrCrCO fragments, respectively.

HOMO-LUMO gaps reflecting electronic stability despite formal unsaturation in the case of **1a**. The Mulliken overlap populations between the metals is 0.06 in **1a** (0.03 in **3a**) whereas it is −0.09 in the Co analog of **1a** in which no metal–metal bond is expected. The principal contributor to the net positive overlap in **1a** and **3a** is from a singly occupied orbital of the two Cp*Cr (or Cp*CrCO) fragments which is basically a metal dz^2 orbital (see Figures 1 and 2, supporting information).[52] The positive combination of these fragments gives rise to MO 40 in **1a** (MO 49 in **3a**) which is Cr–Cr bonding and the negative combination leads to MO 44 (MO 52 in **3a**) which is antibonding. The clean fragment analysis (≈80% of the final MO is derived from this single interaction) supports this interpretation.

The next point concerns how **1** is satisfied with six fewer skeletal electrons than its cobalt analog $Cp_2Co_2B_2H_2S_2$ (known) and $Cp_2Co_2B_4H_8$ (calculated). The two important differences between **1** and its known cobalt analog are the tilted Cp* rings vs coplanar Cp rings in $Cp_2Co_2B_2H_2S_2$[39] and the metal–metal bonding in **1** vs none in the cobalt compound. The LUMO and next two higher MO's for **1a** correspond to the HOMO and next two lower MO's for its Co analog. This is reflected in the MO compositions as well as in their origins in the metal and borane fragments (Figures 3 and 4, supporting information).[52,53] Three occupied cluster orbitals of the cobalt compound are high-lying and empty in **1** and the "t_{2g}" orbitals, which are nonbonding in the cobalt compound, participate in cluster bonding (including the Cr–Cr bond) in **1**. These differences originate in (a) the higher metal based orbital energies of Cr vs Co which bring the "t_{2g}" set into the valence energy regime while raising the energy of other potential cluster orbitals sufficiently such that they remain empty and (b) the nonplanar orientation of the Cp* ligands which breaks the π, δ symmetry of the e_1, e_2 orbital sets of the Cp*M fragment such that the latter can participate in cluster bonding. Concomitantly, in **1a** two of the three "normal" frontier orbitals for a CpM fragment as well as the three "nonbonding t_{2g}" orbitals play a significant role in metal–boron bonding. As a result, no simple isolobal explanation of cluster bonding is apparent.

The third point concerns how **3** accommodates the added pair of electrons relative to **1** thereby becoming saturated. The correlation lines between the MO energies of **1a** and **3a** in Figure 6, which are based on AO and fragment orbital compositions, show that the LUMO of **1a** becomes the HOMO of **3a**. Not shown on the diagram is the fact that two lower lying filled MO's associated with Cr–H–B interactions (apparently MO 25 and 27 although there is no clean 1:1 correspondence) in **1a** are missing from the filled MO set of **3a**. The additional pair of electrons of **3a** is thereby accommodated in one of the empty cluster orbitals of **1**. In terms of electron bookkeeping, of the eight electrons "produced" (2 Cr–H–B orbitals emptied, 2 CO ligands added) two of the electrons go with the 2 H atoms lost, two occupy the former LUMO of **1a**, and four fill the Cr–CO bonding orbitals.

The origin of the stabilization of the additional cluster orbital in **3a** becomes clear on consideration of the effects of adding a CO ligand to a CpM fragment.[54] By virtue of its σ-donor and π-acceptor properties, the single CO ligand strongly splits the Cr 3d based $e_1(\pi)$, $e_2(\delta)$ sets of the CpM fragment. As a consequence, empty cluster MO 42 in **1a** (the LUMO) is sufficiently stabilized such that it becomes filled cluster MO 50 (the HOMO) in **3a**.[55]

The charge distribution on these molecules is the expected one. The overall Mulliken charge on the borane fragment is −1.9 for **1a** (−1.7 for its Co analog) and −2.0 for **3a**. The charge on each Cr atom is 1.5 for **1a** and 1.4 for **3a**. The calculated charges suggest formal Cr(II) d^4 metal centers in both cases. Presumably the molecules are diamagnetic with a

(52) Albright, T. A.; Burdett, J. K.; Whangbo, H.-H. *Orbital Interactions in Chemistry*; Wiley: New York, 1985.

(53) To appreciate the latter point, the nature of the fragment orbitals need be reviewed. The normal frontier orbitals of a CpM fragment are the $2a_1$ and e_1 orbitals which have σ and π symmetry, respectively, with respect to the C_5 axis. The lower lying $1a_1$ and e_2 orbitals, the latter having δ symmetry with respect to the C_5 axis, are normally treated as nonbonding and related to the t_{2g} symmetry orbitals of an octahedral metal center. For Co, the e_1 pair contains 2 electrons and CpCo is viewed as a three-orbital two-electron fragment isolobal with BH. For Cr, the formal frontier orbitals are empty and the "nonbonding" $1a_1$ orbital is singly occupied and, hence, it is viewed as a −1 electron fragment.

(54) The frontier orbitals for a CpMCO fragment are also well-known and a comparison of CpCr and CpCrCO is illustrated in Figure 2, supporting information.

(55) Another difference originates in the changes in the orbitals of the B_4H_8 fragment when two H's are removed. The resulting destabilized fragment orbitals are involved in Cr–H–B bridging interactions in **1a** and two of these are missing in **3a**. This is not to say that the Cr–B unbridged edges are nonbonding. In fact the Cr–B overlap population increases from 0.049 to 0.146 when the bridging hydrogen is removed in going from **1a** to **3a** (Table 2, supporting information).

Chart 1

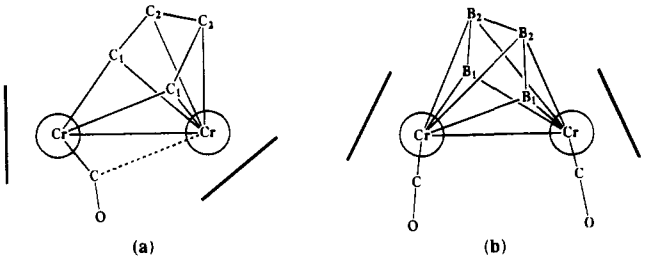

substantial HOMO-LUMO gap because they contain both a direct Cr−Cr interaction and an indirect Cr−Cr interaction via the tetraborane bridge.

Discussion

Comparison of the two pairs of new compounds $Cp^*_2Cr_2B_4H_8$ (**1**), $Cp^*_2Cr_2(CO)_2B_4H_6$ (**3**) and $Cp^*_2Cr_2(BH_4)_2$ (**2**), $Cp^*_2Cr_2(CO)_4(BH_4)_2$ (**4**) contrasts two essentially different unsaturated−saturated electronic systems containing the same principal elements. The paramagnetic chromaborane **2** can be viewed as a bridged dimer of two 14-electron metal centers. The $[BH_4]^-$ ligand is acting as a pseudohalide and **2** is analogous to $[Cp^*CrCl]_2$. The complication of any Cr−Cr bonding interaction is ignored in this description but compound **2** is certainly unsaturated based on the 18-electron rule. Addition of CO results in diamagnetic **4** with Cr atoms that now satisfy the 18-electron rule in a molecule that remains dimeric. On the other hand, diamagnetic chromaborane **1**, with 10 skeletal electrons, is unsaturated relative to the skeletal electron count of 12 associated with the bicapped tetrahedral geometry displayed by **1**. In the presence of the ligand CO, diamagnetic **3** is formed with an increased skeletal electron count of 12 making it saturated with respect to the observed, unchanged bicapped tetrahedral cluster geometry.

It is significant that the unsaturation of **1** resides in the cluster bonding network rather than in a more localized multiple bond. In fact, a closely related organometallic compound containing Cr appears to differ in just this sense. The fragment B_4H_8 is isoelectronic with the fragment C_4H_4 and the 44 cluster valence electron $[Cp_2Cr_2(CO)(C_4Ph_4)]$[56] is analogous to 44 cve **3** to which it is compared in Chart 1. In terms of geometry only, both $[Cp_2Cr_2(CO)(C_4Ph_4)]$ and **3** can be viewed as 6-atom nido structures based on a pentagonal bipyramid with an apical vertex unoccupied in the former case and an equatorial vertex unoccupied in the latter. The orientation of the Cp and Cp* ligands and the positioning of the bridging E_4 fragments, E = C, B, in each case are appropriate to this view. But if one views the CpCr fragment conventionally (formal −1 donor to cluster bonding) each compound lacks 4 electrons of the 16 required for cluster bonding. Based on the observed d_{Cr-Cr} = 2.337(2) Å, the response of $[Cp_2Cr_2(CO)(C_4Ph_4)]$ to the electron deficiency is to form a Cr−Cr triple bond. In contrast, the structural response of **3** is to form a more condensed cluster with a long Cr−Cr bonding interaction that places two of the boron fragments into a capping relationship with respect to a Cr_2B_2 tetrahedron. That is, as evidenced by the shorter pair of Cr−E distances in each case, the primary four atom unit in $[Cp_2Cr_2(CO)(C_4Ph_4)]$ is $Cr_2(C_1)_2$ whereas it is $Cr_2(B_2)_2$ in **3** (see Chart 1). Presumably the different manner in which these two analogous compounds respond to the same number of available skeletal electrons reflects the differences in carbon and boron as well as the greater number of CO ligands and presence of bridging hydrogens in the case of **3**.

The comparison of $[Cp_2Cr_2(CO)(C_4Ph_4)]$ and **3** is of additional interest as we have pointed out previously that the structure of a boron compound serves as a rational model of a less stable structure for its carbon analog and vice versa.[57] Indeed, the rapid racemization of $Fe_2(CO)_6(C_6H_8O_2)$, which possesses a structure analogous to that in Chart 1a, has been suggested to proceed via an intermediate structure analogous to that shown in Chart 1b.[58,59]

Acknowledgment. The support of National Science Foundation is gratefully acknowledged.

Supporting Information Available: Tables 5 and 7 with positional and equivalent isotropic thermal parmeters for **1** and **3**, listing of crystal data, experimental details, crystal data, atomic positional and displacement parameters, full list of distances and bond angles, and least squares planes for **3**, and figures and tables from the MO calculations (17 pages); listing of structure factors (5 pages). This material is contained in many libraries on microfiche, immediately follows this article in the microfilm version of the journal, can be ordered from the ACS, and can be downloaded from the Internet; see any current masthead page for ordering information and Internet access instructions.

JA951791L

(56) Knox, S. A. R.; Stansfield, R. F. D.; Stone, F. G. A.; Winter, M. J.; Woodward, P. *J. Chem. Soc., Dalton Trans.* **1982**, 173.

(57) Dutta, T. K.; Vites, J. V.; Jacobsen, G. B.; Fehlner, T. P. *Organometallics* **1987**, *6*, 842.

(58) Case, R.; Jones, E. R. H.; Schwarz, N. V.; Whing, M. C. *Proc. Chem. Soc., London* **1962**, 256.

(59) Thorn, D. L.; Hoffmann, R. *Inorg. Chem.* **1978**, *17*, 126.